

Diastereoselective Formation of Glycoluril Dimers: Isomerization Mechanism and Implications for Cucurbit[*n*]uril Synthesis

Arindam Chakraborty,[†] Anxin Wu,^{†,‡} Dariusz Witt,^{†,§} Jason Lagona,[†]
James C. Fettinger,[†] and Lyle Isaacs^{*,†}

Contribution from the Department of Chemistry and Biochemistry, University of Maryland,
College Park, College Park, Maryland 20742, and National Laboratory of Applied Organic
Chemistry, Lanzhou University, Lanzhou 730000, P. R. China

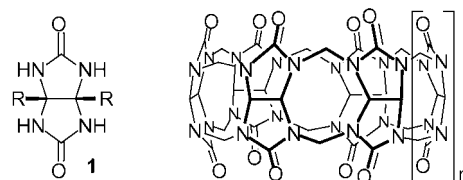
Received February 8, 2002

Abstract: Cucurbit[6]uril (**CB**[6]) is a macrocyclic compound, prepared in one pot from glycoluril and formaldehyde, whose molecular recognition properties have made it the object of intense study. Studies of the mechanism of **CB**[*n*] formation, which might provide insights that allow the tailor-made synthesis of **CB**[*n*] homologues and derivatives, have been hampered by the complex structure of **CB**[*n*]. By reducing the complexity of the reaction to the formation of S-shaped (**12S**–**18S**) and C-shaped (**12C**–**18C**) methylene bridged glycoluril dimers, we have been able to probe the fundamental steps of the mechanism of **CB**[*n*] synthesis to a level that has not been possible previously. For example, we present strong evidence that the mechanism of **CB**[*n*] synthesis proceeds via the intermediacy of both S-shaped and C-shaped dimers. The first experimental determination of the relative free energies of the S-shaped and C-shaped dimers indicates a thermodynamic preference (1.55–3.25 kcal mol⁻¹) for the C-shaped diastereomer. This thermodynamic preference is not because of self-association, solvation, or template effects. Furthermore, labeling experiments have allowed us to elucidate the mechanism of this acid-catalyzed equilibrium between the S-shaped and C-shaped diastereomers. The equilibration is an intramolecular process that proceeds with high diastereoselectivity and retention of configuration. On the basis of the broad implications of these results for **CB**[*n*] synthesis, we suggest new synthetic strategies that may allow for the improved preparation of **CB**[*n*] (*n* > 8) and **CB**[*n*] derivatives from functionalized glycolurils.

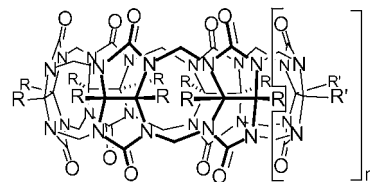
Introduction

In 1905, Behrend reported that the condensation reaction of glycoluril (**1a**) and formaldehyde in concentrated HCl yields an insoluble polymeric material.¹ To make the material more tractable, it was dissolved in concentrated sulfuric acid from which a crystalline substance could be obtained. In 1981, Mock et al.² reinvestigated Behrend's original report and discovered that the product of this reaction was cucurbituril, **CB**[6],³ a remarkable macrocyclic compound comprising six glycoluril rings and 12 methylene bridges (Chart 1). In their syntheses of **CB**[6], neither Behrend nor Mock detected the presence of macrocyclic compounds comprising five, seven, or eight glycoluril rings (**CB**[5], **CB**[7], **CB**[8]). This result, when coupled with the high yield (82%) synthesis of **CB**[6] disclosed by Buschmann, suggested that the formation of **CB**[6] was

Chart 1



- | | |
|--|--------------------------------|
| 1a R = H | CB [5] (<i>n</i> = 0) |
| 1b R = Me | CB [6] (<i>n</i> = 1) |
| 1c R,R' = (CH ₂) ₄ | CB [7] (<i>n</i> = 2) |
| 1d R = Ph | CB [8] (<i>n</i> = 3) |
| 1e R = CO ₂ Et | CB [10] (<i>n</i> = 5) |



- | |
|---|
| Me ₆ CB [5] (R = R' = Me, <i>n</i> = 0) |
| Cy ₅ CB [5] (R,R' = R',R' = (CH ₂) ₄ , <i>n</i> = 0) |
| Cy ₆ CB [6] (R,R' = R',R' = (CH ₂) ₄ , <i>n</i> = 1) |
| Ph ₂ CB [6] (R = H, R' = Ph, <i>n</i> = 1) |

* To whom correspondence should be addressed. E-mail: LI8@umail.umd.edu.

[†] University of Maryland.

[‡] Lanzhou University.

[§] Current address: Chemical Faculty, Technical University of Gdansk, Narutowicza 11/12, 80-952 Gdansk, Poland.

- Behrend, R.; Meyer, E.; Rusche, F. *Liebigs Ann. Chem.* **1905**, 339, 1–37.
- Freeman, W. A.; Mock, W. L.; Shih, N. Y. *J. Am. Chem. Soc.* **1981**, 103, 7367–8.
- Kim, J.; Jung, I.-S.; Kim, S.-Y.; Lee, E.; Kang, J.-K.; Sakamoto, S.; Yamaguchi, K.; Kim, K. *J. Am. Chem. Soc.* **2000**, 122, 540–541.

governed by a thermodynamic preference for **CB**[6].⁴ The first successful synthesis of an analogue of **CB**[6] was described by

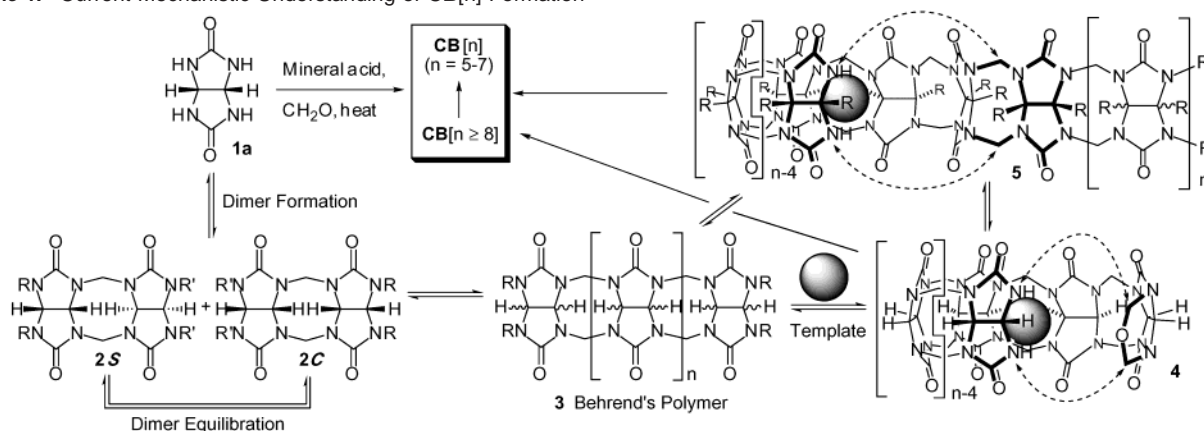
Stoddart who found that the condensation reaction between dimethylglycoluril **1b** and formaldehyde gives rise to cyclic pentameric Me₁₀CB[5].⁵ Again, cyclic oligomers containing larger or smaller numbers of equivalents of **1b** were not detected. The belief that only a single cyclic oligomer would be accessible by the acid-catalyzed condensation reaction gained further acceptance following the suggestion by Cintas that “glycoluril directs the formation of the product and participates in the macroscopic geometry, although in this case, the template is an integral part of the structure it helps to form.”⁶ Since 1981, the outstanding molecular recognition properties of CB[6] have been described in numerous reports from the groups of Mock,⁷ Buschmann,⁸ Kim,⁹ and others.^{10–16} In light of the wide range

of recognition properties of CB[6], many researchers have been interested in preparing derivatives of cucurbituril comprising different numbers of glycoluril rings, containing complex functional groups on their convex face, and whose methylene bridges are functionalized. Success in these endeavors has recently started to appear in the literature.^{3,17–23}

Concurrent with our preliminary report²⁴ on the diastereoselective formation of methylene bridged glycoluril dimers, the groups of Kim^{3,21} and Day^{17–19} reported the preparation and characterization of homologues of cucurbituril containing five, seven, eight, and 10 glycoluril rings (CB[5], CB[7], CB[8], and CB[10]) under strongly acidic conditions (concentrated mineral acids) at moderate temperatures (75–100 °C). Kim recently extended the family of CB[n] to include Cy₅CB[5] and Cy₆CB[6] by the use of **1c** in the condensation process,²² and Nakamura was able to isolate the partially substituted Ph₂CB[6].²³ These new CB[n]s possess remarkable molecular recognition properties^{12,25–27} that have resulted in the synthesis of molecular Russian dolls,²⁸ ball bearings,²⁰ gyroscopes,¹⁷ allowed the selective recognition of a charge-transfer complex,²⁹ and the catalysis of a [2 + 2] photoreaction.³⁰ Clearly, these synthetic and mechanistic studies are expanding the range of CB[n] derivatives that can be accessed and are beginning to define the scope and limitations of the cucurbituril synthesis.

The current state-of-the-art concerning the mechanism of CB[n] synthesis outlined in Scheme 1 largely follows the suggestions of Day et al.¹⁸ The initial condensation of glycoluril with formaldehyde most likely yields a diastereomeric mixture of methylene bridged glycoluril dimers (**2S** and **2C**).^{24,31} We refer to these molecules as S-shaped and C-shaped, respectively, because three-dimensional depictions of these molecules resemble those letters (Chart 2). Depending on the specific conditions of the reaction, **2S** and **2C** may either equilibrate with one another or undergo further oligomerization to yield a diastereomeric mixture (**3**) of glycoluril derivatives with both S- and C-shaped methylene bridged glycoluril dimer substructures. This material, presumably related to Behrend's polymer, must now undergo equilibration to afford oligomers (**4** and **5**) containing stretches of methylene bridged dimers with the all C-shaped relative stereochemistry. This equilibration reaction

- (4) Buschmann, H.-J.; Fink, H.; Schollmeyer, E. Preparation of Cucurbituril. German Patent DE 196 03 377 A1, 1997.
- (5) Flinn, A.; Hough, G. C.; Stoddart, J. F.; Williams, D. *J. Angew. Chem., Int. Ed. Engl.* **1992**, *31*, 1475–1477.
- (6) Cintas, P. *J. Inclusion Phenom. Mol. Recognit. Chem.* **1994**, *17*, 205–20.
- (7) Mock, W. L.; Shih, N. Y. *J. Org. Chem.* **1983**, *48*, 3618–3819. Mock, W. L.; Irra, T. A.; Wepsiec, J. P.; Manimaran, T. L. *J. Org. Chem.* **1983**, *48*, 3619–3620. Mock, W. L.; Shih, N. Y. *J. Org. Chem.* **1986**, *51*, 4440–4446. Mock, W. L.; Shih, N. Y. *J. Am. Chem. Soc.* **1988**, *110*, 4706–4710. Mock, W. L.; Irra, T. A.; Wepsiec, J. P.; Adhya, M. *J. Org. Chem.* **1989**, *54*, 5302–5308. Mock, W. L.; Shih, N. Y. *J. Am. Chem. Soc.* **1989**, *111*, 2697–2699. Mock, W. L.; Pierpont, J. *J. Chem. Soc., Chem. Commun.* **1990**, 1509–1511.
- (8) Buschmann, H. J.; Cleve, E.; Schollmeyer, E. *Inorg. Chim. Acta* **1992**, *193*, 93–97. Buschmann, H. J.; Schollmeyer, E. *Textilveredlung* **1993**, *28*, 182–184. Buschmann, H. J.; Schollmeyer, E. *J. Inclusion Phenom. Mol. Recognit. Chem.* **1997**, *29*, 167–174. Meschke, C.; Buschmann, H. J.; Schollmeyer, E. *Thermochim. Acta* **1997**, *297*, 43–48. Buschmann, H. J.; Jansen, K.; Schollmeyer, E. *Thermochim. Acta* **1998**, *317*, 95–98. Buschmann, H. J.; Jansen, K.; Meschke, C.; Schollmeyer, E. *J. Solution Chem.* **1998**, *27*, 135–140. Buschmann, H. J.; Jansen, K.; Schollmeyer, E. *J. Inclusion Phenom. Macrocyclic Chem.* **2000**, *37*, 231–236. Buschmann, H. J.; Jansen, K.; Schollmeyer, E. *Thermochim. Acta* **2000**, *346*, 33–36. Buschmann, H. J.; Cleve, E.; Jansen, K.; Wego, A.; Schollmeyer, E. *J. Inclusion Phenom. Macrocyclic Chem.* **2001**, *40*, 117–120. Buschmann, H. J.; Cleve, E.; Jansen, K.; Schollmeyer, E. *Anal. Chim. Acta* **2001**, *437*, 157–163. Jansen, K.; Buschmann, H. J.; Wego, A.; Dopp, D.; Mayer, C.; Drexler, H. J.; Holdt, H. J.; Schollmeyer, E. *J. Inclusion Phenom. Macrocyclic Chem.* **2001**, *39*, 357–363.
- (9) Kim, H.-J.; Jeon, Y.-M.; Kim, J.; Whang, D.; Kim, K. *J. Am. Chem. Soc.* **1996**, *118*, 9790–9791. Whang, D.; Heo, J.; Park, J. H.; Kim, K. *Angew. Chem., Int. Ed.* **1998**, *37*, 78–80. Whang, D.; Park, K.-M.; Heo, J.; Ashton, P.; Kim, K. *J. Am. Chem. Soc.* **1998**, *120*, 4899–4900. Whang, D.; Jeon, Y.-M.; Heo, J.; Kim, K. *J. Am. Chem. Soc.* **1996**, *118*, 11333–11334. Roh, S.-G.; Park, K.-M.; Park, G.-J.; Sakamoto, S.; Yamaguchi, K.; Kim, K. *Angew. Chem., Int. Ed.* **1999**, *38*, 638–641. Park, K.-M.; Whang, D.; Lee, E.; Heo, J.; Kim, K. *Chem.-Eur. J.* **2002**, *8*, 498–508. Lee, J. W.; Ko, Y. H.; Park, S.-H.; Yamaguchi, K.; Kim, K. *Angew. Chem., Int. Ed.* **2001**, *40*, 746–749. Lee, E.; Heo, J.; Kim, K. *Angew. Chem., Int. Ed.* **2000**, *39*, 2699–2701. Kim, S.-Y.; Jung, I.-S.; Lee, E.; Kim, J.; Sakamoto, S.; Yamaguchi, K.; Kim, K. *Angew. Chem., Int. Ed.* **2001**, *40*, 2119–2121. Isobe, H.; Tomita, N.; Lee, J. W.; Kim, H.-J.; Kim, K.; Nakamura, E. *Angew. Chem., Int. Ed.* **2000**, *39*, 4257–4260. El Haouaj, M.; Luhmer, M.; Ko, Y. H.; Kim, K.; Bartik, K. *J. Chem. Soc., Perkin Trans. 2* **2001**, 804–807. El Haouaj, M.; Young, H. K.; Luhmer, M.; Kim, K.; Bartik, K. *J. Chem. Soc., Perkin Trans. 2* **2001**, 2104–2107.
- (10) Karcher, S.; Kormmuller, A.; Jekel, M. *Water Sci. Technol.* **1999**, *40*, 425–433. Karcher, S.; Kormmuller, A.; Jekel, M. *Acta Hydrochim. Hydrobiol.* **1999**, *27*, 38–42. Karcher, S.; Kormmuller, A.; Jekel, M. *Water Res.* **2001**, *35*, 3309–3316.
- (11) Sokolov, M. N.; Virovets, A. V.; Dybtsev, D. N.; Gerasko, O. A.; Fedin, V. P.; Hernandez-Molina, R.; Clegg, W.; Sykes, A. G. *Angew. Chem., Int. Ed.* **2000**, *39*, 1659–1661. Fedin, V. P.; Sokolov, M.; Lamprecht, G. J.; Hernandez-Molina, R.; Seo, M.-S.; Virovets, A. V.; Clegg, W.; Sykes, A. G. *Inorg. Chem.* **2001**, *40*, 6598–6603. Fedin, V. P.; Gramlich, V.; Woerle, M.; Weber, T. *Inorg. Chem.* **2001**, *40*, 1074–1077. Sokolov, M. N.; Virovets, A. V.; Dybtsev, D. N.; Chubarova, E. V.; Fedin, V. P.; Fenske, D. *Inorg. Chem.* **2001**, *40*, 4816–4817.
- (12) Marquez, C.; Nau, W. M. *Angew. Chem., Int. Ed.* **2001**, *40*, 4387–4390. Marquez, C.; Nau, W. M. *Angew. Chem., Int. Ed.* **2001**, *40*, 3155–3160.
- (13) Tuncel, D.; Steinke, J. H. G. *Chem. Commun.* **1999**, 1509–1510. Tuncel, D.; Steinke, J. H. G. *Chem. Commun.* **2001**, 253–254. Krasia, T. C.; Steinke, J. H. G. *Chem. Commun.* **2002**, 22–23.
- (14) Hoffmann, R.; Knoche, W.; Fenn, C.; Buschmann, H.-J. *J. Chem. Soc., Faraday Trans.* **1994**, *90*, 1507–1511. Neugebauer, R.; Knoche, W. *J. Chem. Soc., Perkin Trans. 2* **1998**, 529–534.
- (15) Wagner, B. D.; MacRae, A. I. *J. Phys. Chem. B* **1999**, *103*, 10114–10119. Wagner, B. D.; Fitzpatrick, S. J.; Gill, M. A.; MacRae, A. I.; Stojanovic, N. *Can. J. Chem.* **2001**, *79*, 1101–1104.
- (16) Zhang, X. X.; Krakowiak, K. E.; Xue, G.; Bradshaw, J. S.; Izatt, R. M. *Ind. Eng. Chem. Res.* **2000**, *39*, 3516–3520.
- (17) Day, A. I.; Blanch, R. J.; Arnold, A. P.; Lorenzo, S.; Lewis, G. R.; Dance, I. *Angew. Chem., Int. Ed.* **2002**, *41*, 275–277.
- (18) Day, A.; Arnold, A. P.; Blanch, R. J.; Snushall, B. *J. Org. Chem.* **2001**, *66*, 8094–8100.
- (19) Day, A. I.; Arnold, A. P.; Blanch, R. J. Method for Synthesis Cucurbiturils. PCT Intl. Appl. PCT/AU00/00412, 2000.
- (20) Blanch, R. J.; Sleeman, A. J.; White, T. J.; Arnold, A. P.; Day, A. I. *Nano Lett.* **2002**, *2*, 147–149.
- (21) Kim, K.; Kim, J.; Jung, I.-S.; Kim, S.-Y.; Lee, E.; Kang, J.-K. Cucurbituril Derivatives, Their Preparation and Uses. European Patent Appl. EP 1 094 065 A2, 2001.
- (22) Zhao, J.; Kim, H.-J.; Oh, J.; Kim, S.-Y.; Lee, J. W.; Sakamoto, S.; Yamaguchi, K.; Kim, K. *Angew. Chem., Int. Ed.* **2001**, *40*, 4233–4235.
- (23) Isobe, H.; Sato, S.; Nakamura, E. *Org. Lett.* **2002**, *4*, 1287–1289. For another report of partially substituted CB[n], see ref 19.
- (24) Witt, D.; Lagona, J.; Damkaci, F.; Fettingner, J. C.; Isaacs, L. *Org. Lett.* **2000**, *2*, 755–758.
- (25) Kim, H.-J.; Jeon, W. S.; Ko, Y. H.; Kim, K. *Proc. Natl. Acad. Sci. U.S.A.* **2002**, *99*, 5007–5011.
- (26) Ong, W.; Gómez-Kaifer, M.; Kaifer, A. E. *Org. Lett.* **2002**, *4*, ASAP.
- (27) Lorenzo, S.; Day, A.; Craig, D.; Blanch, R.; Arnold, A.; Dance, I. *CrystEngComm* **2001**, *49*, 1–7.
- (28) Kim, S.-Y.; Jung, I.-S.; Lee, E.; Kim, J.; Sakamoto, S.; Yamaguchi, K.; Kim, K. *Angew. Chem., Int. Ed.* **2001**, *40*, 2119–2121.
- (29) Kim, H.-J.; Heo, J.; Jeon, W. S.; Lee, E.; Kim, J.; Sakamoto, S.; Yamaguchi, K.; Kim, K. *Angew. Chem., Int. Ed.* **2001**, *40*, 1526–1529.
- (30) Jon, S. Y.; Ko, Y. H.; Park, S. H.; Kim, H.-J.; Kim, K. *Chem. Commun.* **2001**, 1938–1939.
- (31) Wu, A.; Chakraborty, A.; Witt, D.; Lagona, J.; Damkaci, F.; Ofori, M.; Chiles, K.; Fettingner, J. C.; Isaacs, L. *J. Org. Chem.* **2002**, *67*, in press.

Scheme 1. Current Mechanistic Understanding of $\text{CB}[n]$ Formation^a

^a The dashed arrows indicate C–N bonds that need to be formed to yield $\text{CB}[n]$.

may, or may not, be influenced by the presence of appropriate templating molecules in the reaction medium. Day recently reported modest effects of acid type, acid concentration, reactant concentration, temperature, templating molecules, anions, and cations on the distribution of $\text{CB}[n]$ obtained in the condensation reaction.^{18,19} These oligomeric intermediates, **4** and **5**, then undergo cyclization reactions to enter the $\text{CB}[n]$ manifold. Day also demonstrated, by elegant product resubmission experiments, that within the $\text{CB}[n]$ manifold pure $\text{CB}[8]$ is converted under the reaction conditions (concentrated HCl, 100 °C) to $\text{CB}[5]$, $\text{CB}[6]$, and $\text{CB}[7]$, but that $\text{CB}[5]$, $\text{CB}[6]$, and $\text{CB}[7]$ are stable under these conditions.¹⁸

The complexity associated with the $\text{CB}[n]$ synthesis – formation of n rings, $2n$ methylene bridges, with complete control over the relative stereochemistry of n glycoluril rings – has frustrated experimental attempts to (1) obtain proof of the intermediacy of glycoluril dimers with the relative stereochemistry exemplified by **2S**, (2) assess the relative thermodynamic stability of **2S** and **2C**, and (3) elucidate the mechanism for the interconversion of **2S** and **2C**. Our approach to the synthesis of analogues of $\text{CB}[6]$ and other glycoluril derivatives with interesting molecular recognition properties^{32,33} relies on the identification of the methylene bridged glycoluril dimer substructure (**2C**) as the fundamental building block of $\text{CB}[n]$. Previously, we described three complementary synthetic methods that allow for the efficient synthesis of methylene bridged glycoluril dimers bearing two *o*-xylylene substituents (Chart 2). As a result of this synthetic simplification, the complexity of the reaction – the formation of one ring, two methylene bridges, and control over the relative stereochemistry of two glycoluril rings – was substantially reduced relative to the synthesis of $\text{CB}[n]$. As a result, we have been able to address several key mechanistic questions that have been elusive in the chemistry of $\text{CB}[n]$ itself. In this paper, we discuss (1) the kinetic (S- and C-shaped) and thermodynamic (C-shaped) products of the dimerization reaction, (2) the ratio of the S- and C-shaped methylene bridged glycoluril dimers under equilibrium conditions, (3) potential sources of the observed preference for the C-shaped diastereomer, and (4) the mechanism of the isomerization of the S- to the C-shaped dimers. Last, we discuss the

implication of these results for the synthesis of new derivatives of cucurbituril.

Results and Discussion

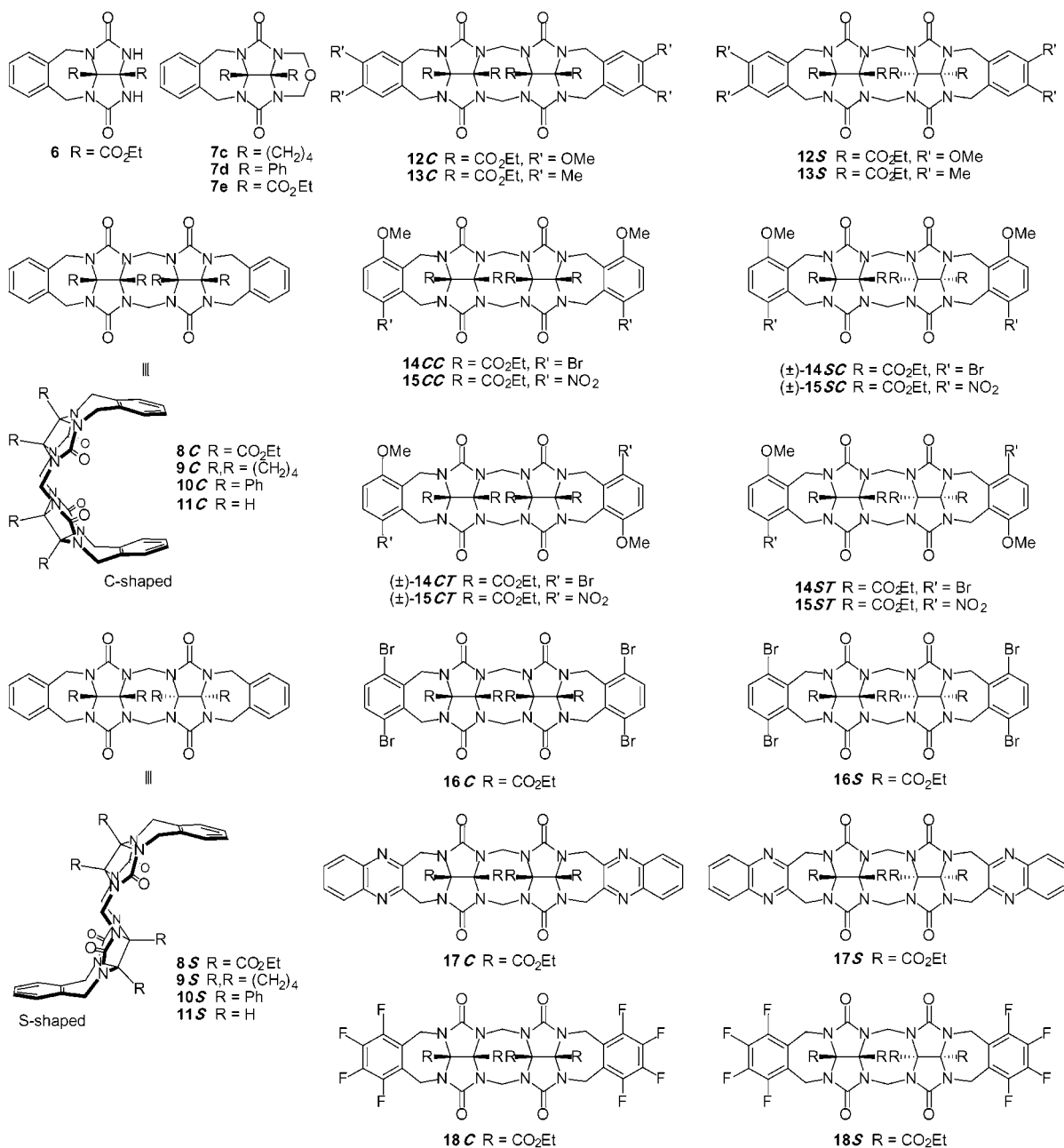
Previously, we reported the synthesis of a wide variety of C-shaped and S-shaped methylene bridged glycoluril dimers.³¹ Chart 2 shows the structures of the compounds that we discuss in this paper. The reaction between glycoluril derivatives **6** and **7** should give rise to roughly equal amounts of S- and C-shaped methylene bridged glycoluril dimers, because the first bond-forming (stereochemical determining) step is unlikely to be highly diastereoselective.³¹ We were surprised, therefore, that condensation reactions typically produced the C-shaped dimers in modest to high diastereoselectivity after 24 h.

Kinetic Formation of a Mixture of C-Shaped and S-Shaped Methylene Bridged Glycoluril Dimers. The diastereoselective formation of C-shaped methylene bridged glycoluril dimers, typified by **8C**, suggested that thermodynamic preferences were playing a major role in the outcome of the reactions. We hypothesized that both the S- and the C-shaped diastereomers were kinetic products that were transformed into the C-shaped diastereomers under thermodynamically controlled conditions. To test this hypothesis, we performed dimerization reactions at lower temperatures and/or with shorter reaction times (Scheme 2). We choose these dimerization reactions because they represent the three different synthetic methods that we have developed and because we were not able to isolate the S-shaped diastereomers when the reactions were run to completion.³¹ Gratifyingly, we found that compound **6** yields a mixture of **7e** (51%), **8C** (37%), and **8S** (7%) when the dimerization reaction is run for only 14 h; **8C** is formed in 88% yield as the only isolable product when the reaction is run to completion. Cyclic ether **19**, for example, is transformed into a 2:3 mixture of **12S** and **12C** when the reaction is run to 59% conversion. In contrast, **12C** was obtained in 87% yield to the exclusion of **12S** when the reaction is run to completion. Similarly, ureidyl NH compound **20** gave a mixture of cyclic ether **21** (15%), **13S** (7%), and **13C** (44%) under milder conditions. The heterodimerization reaction between (\pm)-**22** and cyclic ether (\pm)-**23** was also successful; we were able to isolate **14ST** (7%), (\pm)-**14SC** (6%), (\pm)-**14CT** (12%), and **14CC** (18%) in addition to unreacted starting materials. The *ST*, *SC*, *CT*, and *CC* descriptors denote the overall shape of the molecule (S-shaped

(32) Isaacs, L.; Witt, D. *Angew. Chem., Int. Ed.* **2002**, *41*, 1905–1907.

(33) Isaacs, L.; Witt, D.; Lagona, J. *Org. Lett.* **2001**, *3*, 3221–3224.

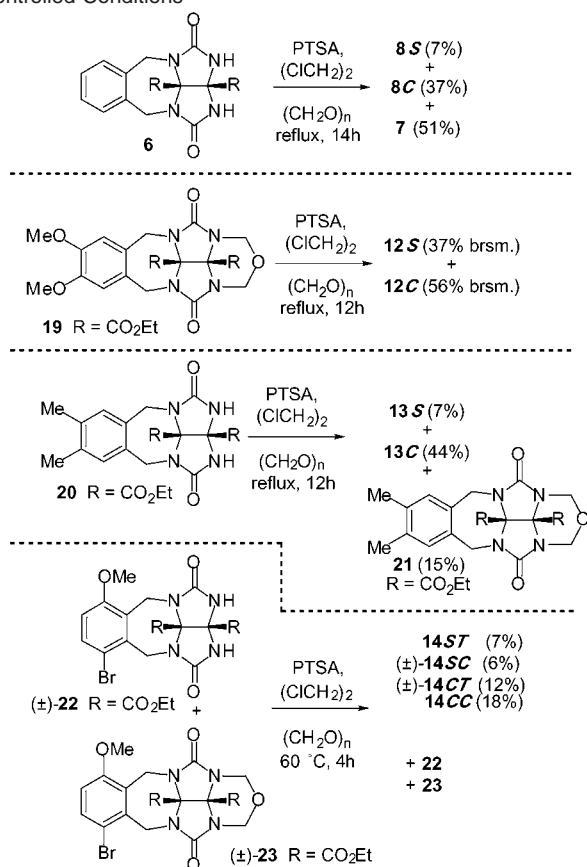
Chart 2. Methylene Bridged Glycoluril Dimers



or C-shaped) and the relative location of the methoxy substituents (cis or trans). A similar reaction with (±)-**22** only yielded the C-shaped compounds (±)-**14CT** (48%) and **14CC** (46%).³¹ These results allow us to conclude that both the C-shaped and the S-shaped diastereomers are kinetic products of the reaction, formed in comparable amounts, whereas the C-shaped diastereomers are the thermodynamic products of the reaction. These results provide strong evidence for the formation of S- and C-shaped methylene bridged glycoluril dimers, **2S** and **2C**, in condensation reactions with formaldehyde and provide experimental support for the suggestion by Day et al.¹⁸ that S-shaped intermediates initially form in the synthesis of **CB[n]**.

Equilibration of S-Shaped and C-Shaped Diastereomers and Determination of Their Relative Free Energies. The previous section demonstrates that both the C- and the S-shaped diastereomers are kinetic products and that the C-shaped diastereomer is the thermodynamic product. Those results do

not, however, allow us to conclude that these reactions have reached thermodynamic equilibrium or to assess the relative free energies of the C- and S-shaped diastereomers. To address these questions, we used the pure C-shaped and S-shaped diastereomers of six different symmetrical homodimers and separately resubmitted them to the reaction conditions (Table 1). If each set of equilibration reactions gives the same C:S ratio, then we can conclude that equilibrium has been reached and calculate a value of ΔG . Table 1 shows that similar C:S ratios were achieved in the majority of cases. Quinoxaline derivatives **17C** and **17S** did not interconvert under the reaction conditions implying that the ~2:1 ratio of **17C**:**17S** obtained in their synthesis represents a slight kinetic preference for **17C**. We attribute the lack of isomerization to preferential protonation of the quinoxaline N-atoms which competes with the protonation of the ureidyl O-atoms required for isomerization. The values of ΔG under the reaction conditions (83 °C) range from -1.55

Scheme 2. Formation of S-Shaped Compounds under Kinetically Controlled Conditions**Table 1.** Equilibration of C- and S-Shaped Compounds^a

starting material	C → C+S C:S	S → C+S C:S	ΔG (kcal mol ⁻¹)
8	98:2	96:4	-2.25 to -2.75
12	98:2	98:2	~ -2.75
13	98:2	97:3	-2.46 to -2.75
16	95:5	90:10	-1.55 to -2.15
17	100:0	0:100	n.e.
18	99:1	98:2	-2.75 to -3.25

^a n.e. = no equilibration.

to -3.25 kcal mol⁻¹. The values of ΔG obtained here represent the first experimental determinations of differences in free energy between S- and C-shaped glycoluril dimers; these values are of fundamental importance toward the synthesis of CB[n] and derivatives. These results suggest that it is the intrinsic preference of the methylene bridged glycoluril dimer substructure to adopt the C-shaped form that drives the formation of CB[n]. It is not necessary, although plausible, to postulate the participation of components of the reaction mixture (glycoluril,

Table 2. Solvent Effects on the **16C:16S** Ratio^a

solvent	C → C+S 16C:16S	S → C+S 16C:16S	ΔΔG (kcal mol ⁻¹)
CHCl ₃	94:6	94:6	-1.83
CCl ₄	99:1	97:3	-2.41 to -3.19
C ₆ F ₆	99:1	97:3	-2.44 to -3.22
THF	100 ^b :0	dec	n.d.
CH ₃ CN	100 ^b :0	98:2	> -2.62
CICH ₂ CH ₂ Cl	95:5	90:10	-1.55 to -2.15
CH ₃ NO ₂	90:10	89:11	-1.55 to -1.63
MeOCH ₂ CH ₂ OMe	97:3	dec	n.d.

^a n.d. = not determined. ^b S-shaped compound not detected. dec = decomposed.

water, salts, or acid) as reaction templates to explain the formation of CB[n] (Scheme 1). A simple calculation, ignoring entropic and enhanced enthalpic contributions in the macrocyclization reaction, suggests that in a worst case scenario (**16C:16S** = 90:10, ΔG = -1.55 kcal mol⁻¹) 53% ((0.9)⁶) of linear glycoluril hexamers would adopt the all C shape needed for CB[6] formation.

Solvent Effects on the C:S Equilibrium. In an attempt to address the factors that influence the relative stability of the C- and S-shaped diastereomers, we performed the isomerization reactions of **16C** and **16S** in a variety of different solvents (Table 2). We hypothesized that different solvents might preferentially solvate either the C-shaped or the S-shaped compounds and thereby influence the C:S ratio at thermodynamic equilibrium. Alternatively, because the S-shaped and C-shaped compounds have different dipole moments, simple changes in the dielectric constant of the medium might influence their ratio at equilibrium. We choose **16C** and **16S** because it was straightforward to prepare sizable quantities of both diastereomers and because the C:S ratio determined in 1,2-dichloroethane would allow us to observe both increases and decreases in the equilibrium ratio. We were unable to study this equilibrium in solvents that undergo destructive side reactions with the iminium ion intermediates (e.g., C₆H₆). Table 2 shows the results of separate equilibration experiments that we performed in eight different solvents; these solvents range in boiling point from 61 °C (CHCl₃) to 101.2 °C (CH₃NO₂), have dielectric constants that range from 2.05 (C₆F₆) to 37.5 (CH₃CN), and display a range of sizes, shapes, and functional groups.^{34,35} As can be seen from Table 2, the effects are neither large, nor do they follow trends based upon the dielectric constant. For example, the smallest **16C:16S** ratio (90:10) was observed in CH₃NO₂ (ε = 35.9), whereas in CH₃CN (ε = 37.5), one of the largest ratios (98:2) was observed. Although we did not observe any dramatic effects attributable to differences in solvation in the solvents studied, we note that the two solvents with the highest **16C:16S** ratios

(34) Laurence, C.; Nicolet, P.; Dalati, M. T.; Abboud, J.-L. M.; Notario, R. *J. Phys. Chem.* **1994**, *98*, 5807–5816.(35) Vogel, A. I.; Furniss, B. S.; Hannaford, A. J.; Smith, P. W. G.; Tatchell, A. R. *Vogel's Textbook of Practical Organic Chemistry*, 5th ed.; Longman Scientific & Technical: Essex, U.K., 1989.

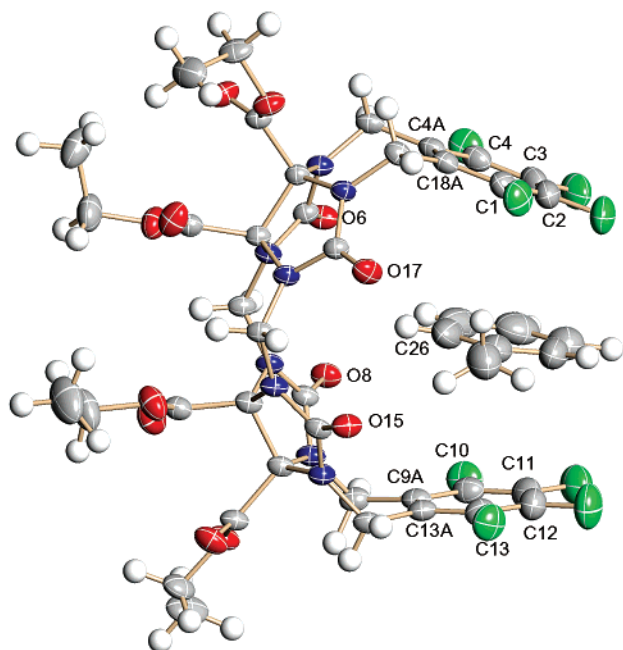


Figure 1. X-ray crystal structure of **18C** as the toluene solvate.

(C_6F_6 and CH_3CN) are those that we would expect to bind within the cleft of **16C**.³¹

The X-ray crystal structure of **18C** (Figure 1) was obtained as the toluene solvate and depicts one possible orientation of an aromatic solvent within the cleft defined by the two tetrafluorophenyl rings. The distance between the tips of the aromatic rings, defined as the distance between the C2–C3 and C11–C12 centroids, is 6.786 Å, which represents a nearly ideal spacing for complexation of an aromatic ring. The distance between the centroids of the two tetrafluorophenyl rings is 7.228 Å. The solvating toluene assumes an offset stacked arrangement with respect to the tetrafluorophenyl rings. It is twisted by approximately 30° with respect to the tetrafluorophenyl rings; the dihedral angles from C26 through the centroids of the toluene ring, the tetrafluorophenyl ring, and the centroids of the C4A–C18A and C9A–C13A bonds amount to 2.0° and –4.9°, respectively. The molecule exhibits a slight end-to-end twist of –3.0° as defined by the dihedral angle through the centroids of the C2–C3, C4A–C18A, C9A–C13A, and C11–C12 bonds. The distances between the carbonyl oxygens of each glycoluril ring, O8–O15 and O6–O17, amount to 5.918 and 5.889 Å, respectively, values slightly smaller than those observed for **CB[6]** (5.98–6.042 Å).²

Self-Association Is Not the Cause of Enhanced C:S Ratios.

One possible explanation for the relatively large C:S ratios is self-association. Nolte has observed a tendency for related molecules to dimerize in $CHCl_3$ and water, and we have observed strong self-association for our C-shaped molecules in water.^{32,33,36–39} Self-association of the C-shaped compounds would sequester them as the dimers resulting in a shift in the

equilibrium toward the C-shaped form. Such an equilibrium shift would, of course, be sensitive to concentration, solvent, temperature, and self-association constant (K_s). At the concentrations at which we perform the condensation reaction – up to 100 mM, but more typically 20 mM – relatively large values of K_s ($>100 M^{-1}$) would be required to drive the equilibrium. To test for self-association, we performed a dilution experiment with **12C** in $ClCD_2CD_2Cl$ ($[12C] = 200 \mu M$ to 100 mM, 298 K). We did not observe any changes in chemical shift over this concentration range, which implies that self-association is negligible for **12C**.⁴⁰ It is unlikely, therefore, that the diastereoselective formation of the C-shaped compounds is due to self-association.

Templation of the C-Shaped Diastereomer by *p*-Toluene-sulfonic Acid Is Not the Cause of Enhanced C:S Ratios.

Another potential cause of the large preference for the C-shaped diastereomers is the templation of the C-shaped compounds by a molecule of PTSA. Binding of PTSA within the C-shaped cavity would result in a shift in the C to S equilibrium in favor of the C-shaped compound. A typical dimerization reaction – the formation of **12C** for example – results in a solution with $[12C] = 20$ mM and $[PTSA] = 100$ mM. For PTSA to bind to and thereby template at least 90% of the molecules of **12C**, a binding constant of $K_a > 109 M^{-1}$ would be required. To test for the possibility that PTSA is acting as a template in this reaction, we performed a titration experiment with **12C** and PTSA in $ClCD_2CD_2Cl$ ($[12C] = 20$ mM, $[PTSA] = 0$ –100 mM, 70 °C). We did not observe changes in chemical shift of the aromatic protons of **12C** suggesting that PTSA does not bind within the cavity of **12C** under these conditions.⁴¹ It is unlikely, therefore, that the diastereoselective formation of the C-shaped compounds is due to PTSA acting as a template.

AM1 Calculations Reveal a Thermodynamic Preference for the C-Shaped Diastereomer.

Having excluded many of the plausible experimental causes of the diastereoselective formation of C-shaped methylene bridged glycoluril dimers, we considered the possibility that the C-shaped diastereomers are simply thermodynamically more stable than the S-shaped diastereomers. For this purpose, we decided to compute the relative heats of formation of the C-shaped and S-shaped diastereomers (Table 3).¹⁸ Table 3 shows AM1 computational results of the heats of formation of **8**–**11**. These computations suggest a small (0.5 kcal mol^{–1}) to a quite large difference (–10.2 kcal mol^{–1}) in the heat of formation between the S- and C-shaped diastereomers. In particular, the difference calculated for ethoxycarbonyl substituted **8** (–10.2 kcal mol^{–1}) is significantly larger than the experimental value (–2.25 to –2.75 kcal mol^{–1}) determined by equilibration studies in $ClCH_2-CH_2Cl$ described above. Given the large differences in the heats

(36) Holder, S. J.; Elemans, J. A. A. W.; Donners, J. J. M.; Boerakker, M. J.; de Gelder, R.; Barbera, J.; Rowan, A. E.; Nolte, R. J. M. *J. Org. Chem.* **2001**, *66*, 391–399.

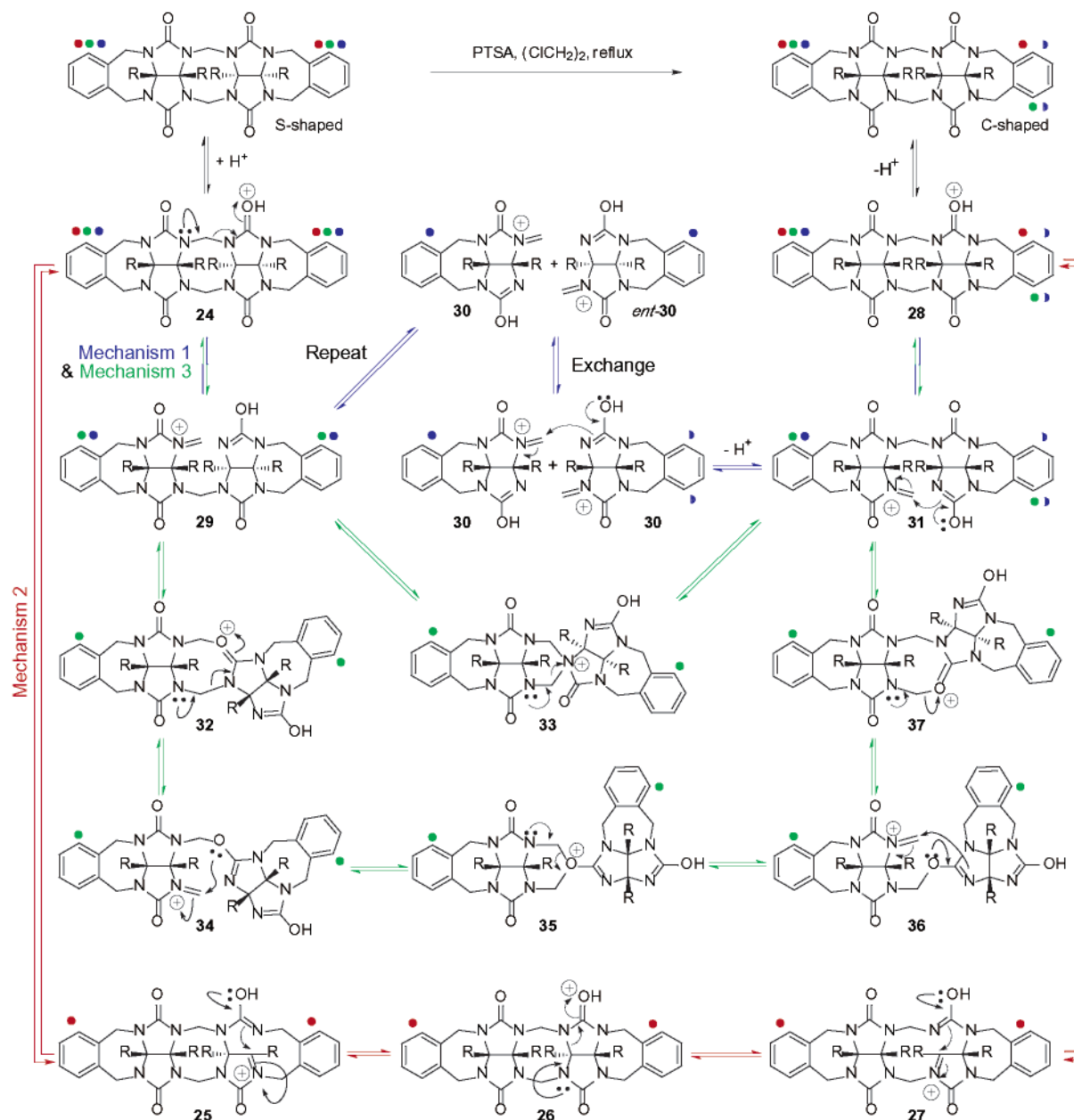
(37) Rowan, A. E.; Elemans, J. A. A. W.; Nolte, R. J. M. *Acc. Chem. Res.* **1999**, *32*, 995–1006.

(38) Elemans, J. A. A. W.; de Gelder, R.; Rowan, A. E.; Nolte, R. J. M. *Chem. Commun.* **1998**, 1553–1554.

(39) Reek, J. N. H.; Kros, A.; Nolte, R. J. M. *Chem. Commun.* **1996**, 245–247. Elemans, J. A. A. W.; Rowan, A. E.; Nolte, R. J. M. *J. Am. Chem. Soc.* **2002**, *124*, 1532–1540.

(40) Alternatively, the observation of no changes in chemical shift could indicate a fully dimeric form over this range of concentration. When we have observed dimers for our compounds, we have invariably observed sizable upfield shifts in the NMR which we do not observe for **12C**. We, therefore, formulate **12C** as the monomer in 1,2-dichloroethane. We have performed similar dilution experiments for **8C**, **12C**, **13C**, **16C**, **17C**, and **18C** in the more economical solvent $CDCl_3$, and, in all cases, the self-association constants ($K_s < 10 M^{-1}$) were too small to be responsible for the predominance of the C-shaped diastereomer.

(41) We did, however, note small changes (~0.04 ppm) in the chemical shift of the protons on the central methylene bridges. These changes are not well described by a 1:1 binding model, but are consistent with a small conformational change of the central eight-membered ring. For a discussion of these types of conformational changes, see: Jansen, R. J.; de Gelder, R.; Rowan, A. E.; Scheeren, H. W.; Nolte, R. J. M. *J. Org. Chem.* **2001**, *66*, 2643–2653.

Scheme 3. Three Different Mechanisms for the Equilibrium between the S- and C-Shaped Diastereomers**Table 3.** AM1 Heats of Formation (kcal mol⁻¹) for **8**–**11**

	ΔH_f° (AM1)		$\Delta\Delta H_f^\circ$ (AM1)
	S-shaped	C-shaped	
8 ^a	–237.7 to –243.8	–246.9 to –250.1	–6.3 to –10.2
9 ^b	47.6/47.3	45.3/45.2	–2.3 to –2.2
10	216.9	211.5	–5.4
11	58.2	58.7	0.5

^a There are many different relative orientations of the four CO₂Et groups.

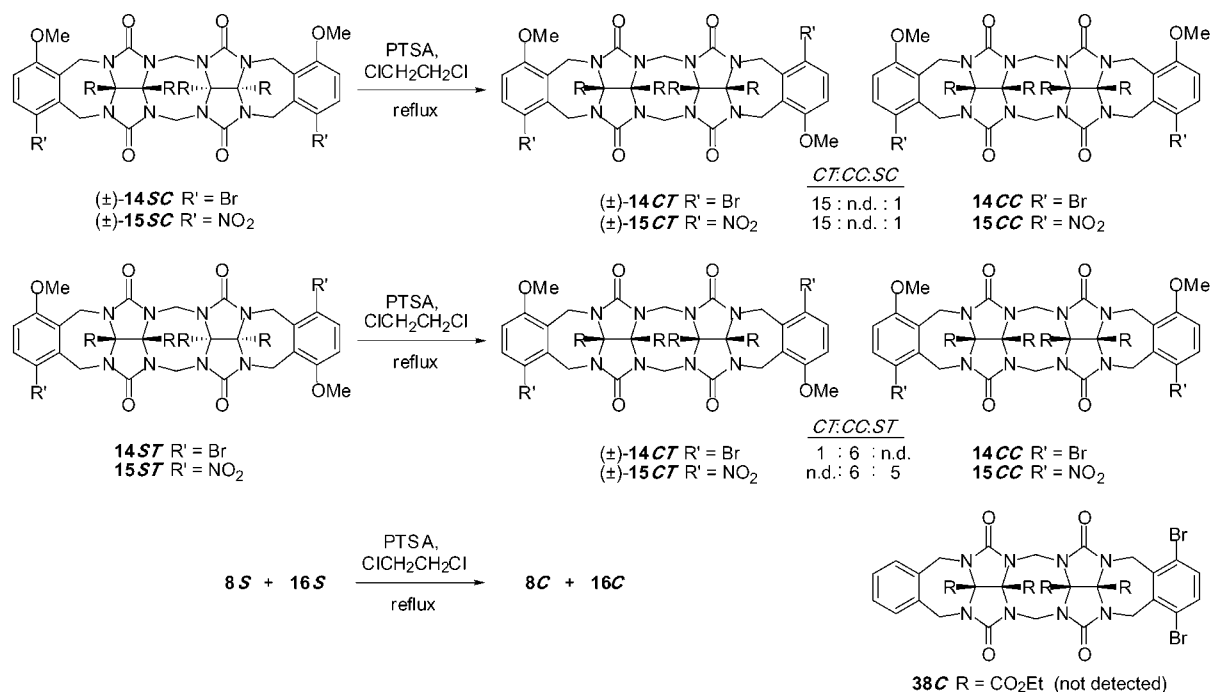
^b Two different relative orientations of the boat-shaped fused six-membered rings are possible.

of formation between the glycoluril dimers bearing different substituents, we are more confident in the experimental relative free energy values given in Table 1.

Mechanism of the Interconversion of the C- and S-Shaped Diastereomers. Previously, we have discussed the mechanism for the formation of methylene bridged glycoluril dimers.³¹ In this section, we discuss experiments that pertain to the mech-

anism of the interconversion between the S- and C-shaped diastereomers. Scheme 3 describes the three different mechanistic proposals; the equilibrium arrows that connect intermediates along a single mechanistic path are color coded (mechanism 1, blue; mechanism 2, red; mechanism 3, green). All three mechanisms begin with protonation of one of the carbonyl oxygens by the acid catalyst (PTSA) giving **24**. From this point the three mechanisms diverge. In mechanism 2, one C–N bond of the glycoluril skeleton breaks, generating intermediate **25**, which has lost one stereogenic center. Reclosure of that same C–N bond can occur to generate intermediate **26**; this two-step process results in net inversion of configuration at that carbon atom. Intermediate **26** is probably prohibitively high in energy because of the trans ring junction, which disfavors mechanism 2. Repetition of this two-step process results in inversion of configuration at the second C-atom delivering intermediate **28** by way of **27**. Intermediate **28** is common to

Scheme 4. Diastereoselective Equilibration Reactions



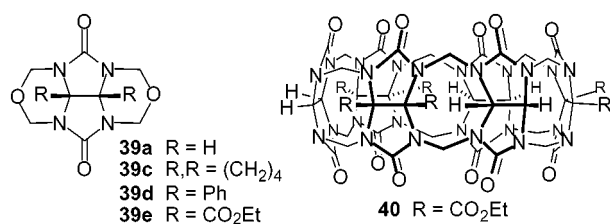
all three mechanisms; upon loss of a proton it delivers the C-shaped diastereomer. Overall, mechanism 2 is an intramolecular process that results in the inversion of configuration at two C-atoms. Mechanisms 1 and 3 diverge from mechanism 2 in the transformation of **24** into **29** by cleavage of one of the C–N bonds of a methylene bridge. Mechanisms 1 and 3 diverge from **29**. Mechanism 1 proceeds by the protonation of **29** followed by cleavage of a second C–N bond of the methylene bridge to yield the pair of intermediates (**30**). We have depicted the cleavage of **29** such that each half retains a single positive charge; the alternative pathway involving one half retaining both methylene bridges and two positive charges is also possible, but likely to be higher in energy. It is worth noting that the pair of intermediates generated in this manner from a single molecule of **29** is heterochiral, that is, the racemic mixture (\pm)-**30**. To generate the C-shaped product, this pair must undergo exchange with other like intermediates to generate the homochiral pair comprising two molecules of **30** or *ent*-**30**. This pair is then able to sequentially reform the C–N bonds of the two methylene bridges forming C-shaped product by way of **31** and common intermediate **28**. Overall, mechanism 1 results in breaking of the S-shaped glycoluril dimer into two heterochiral pieces that undergo exchange to generate a homochiral pair that results in formation of the C-shaped product. Mechanism 3 diverges from mechanism 1 at intermediate **29**. In mechanism 3, the iminium ion intermediate **29** is captured by the carbonyl oxygen lone pair yielding **32** or by the ureidyl nitrogen lone pair yielding intermediate **33**. Of these two options, we prefer the use of the oxygen atom lone pair because it is likely to be more nucleophilic. The overall pathway, however, is better illustrated conceptually via spiro compound **33**. The spiro compound can break down in two ways, one leading back to intermediate **29** and one leading to **31** which after deprotonation yields common intermediate **28** and then the C-shaped diastereomer. The overall process of mechanism 3 results in intramo-

lecular swapping of partner N-atoms involved in the methylene bridges. The use of the oxygen lone pair to accomplish the same overall transformation of **29** into **31** proceeds via intermediates **32** and **34–37**.

Mechanisms 1–3 have different stereochemical outcomes and can be distinguished on the basis of labeling experiments. To schematically illustrate the different outcomes, two different carbon atoms of the starting S-shaped diastereomer (Scheme 3) were labeled with blue, red, and green dots. The positions of these labels are indicated as they progress through mechanisms 1, 2, and 3, respectively. As can be readily ascertained from Scheme 3, mechanism 1 (blue) leads to a scrambling of the label between two locations (blue half circles), mechanism 2 (red) does not result in any change in the relative position (cis) of the labels (red dots), and mechanism 3 (green) results in a transposition of one of the labels to the opposite side (trans) of the C-shaped diastereomer (green dots).

To realize this labeling experiment in practice, we separately performed isomerization reactions of (\pm)-**14SC** and the meso compound **14ST** (Scheme 4). Under mechanism 1, (\pm)-**14SC** should yield a mixture of **14CC** and (\pm)-**14CT**, under mechanism 2 only **14CC**, and under mechanism 3 only (\pm)-**14CT**. Similarly, under mechanism 1, **14ST** would yield a mixture of **14CC** and (\pm)-**14CT**, under mechanism 2 only **14CT**, and under mechanism 3 only **14CC**. Scheme 4 shows the results of the equilibration reactions of (\pm)-**14SC**, **14ST**, (\pm)-**15SC**, and **15ST**. The separate isomerization reactions of (\pm)-**14SC** and (\pm)-**15SC** gave *only* (\pm)-**14CT** and (\pm)-**15CT**, respectively, along with small amounts of unreacted starting material. The isomerization reaction of **14ST** yields **14CC** and (\pm)-**14CT** in a 6:1 ratio, whereas the sluggish isomerization of **15ST** gave exclusively **15CC** at 55% conversion. These results provide strong evidence that mechanism 3 is the dominant pathway for the interconversion of the S-shaped and C-shaped diastereomers under our standard isomerization conditions ($\text{ClCH}_2\text{CH}_2\text{Cl}$, anhydrous

Chart 3



PTSA, reflux). We also performed a crossover experiment involving the isomerization of a mixture of **8S** and **16S**. Under mechanism 1, we would expect the formation of **8C**, **16C**, and the crossover product, heterodimer **38C**. In contrast, if mechanism 3 is dominant, then **8C** and **16C** should be the exclusive products. When this isomerization reaction was run to 78% completion, we observed the clean formation of a mixture of **8C** and **16C** providing additional support for the dominance of mechanism 3.

The fact that the isomerization of methylene bridged glycoluril dimers follows mechanism 3 is not only useful in the synthesis of our compounds, but might be important for the tailored synthesis of **CB**[*n*] and its derivatives. For example, Day and co-workers have recently shown that heating purified **CB**[8] in concentrated HCl at 100 °C results in the formation of **CB**[5], **CB**[6], and **CB**[7]. In contrast, pure **CB**[5], **CB**[6], and **CB**[7] are stable under these conditions.¹⁸ These results require that two adjacent methylene bridges are broken and that one or more glycoluril rings are extruded. This type of reaction would likely follow a pathway related to mechanism 1. We believe that mechanism 1 is not operative in our system because we work under anhydrous acidic conditions. In aqueous acid, it is likely that H₂O can compete with the internal N and O nucleophiles of mechanism 3 for the capture of **29** (Scheme 3), effectively forcing fragmentation of the methylene bridges by a variation of mechanism 1. In the absence of competing nucleophiles, under anhydrous acidic conditions, we suggest that **CB**[*n*] (*n* > 8) and derivatives might display enhanced stability. We further suggest that the optimal synthesis of **CB**[*n*] (*n* > 8) and derivatives might be best performed in a two-step manner similar to our heterodimerization reactions, via reaction of a bis(cyclic ether) (e.g., **39a**–**39e**, Chart 3) and a functionalized glycoluril (e.g., **1a**–**1e**), followed by an isomerization step of the intermediate S- and C-shaped methylene bridged glycoluril oligomers under anhydrous acidic conditions. If this approach is fruitful, it might be possible to prepare **CB**[*n*] derivatives from two different glycoluril derivatives (e.g., **39e** and **1a**), and that those derivatives might alternate in the **CB**[*n*] derivative (e.g., **40**).¹⁹

Conclusions

Until recently, it has not been possible to prepare either homologues or derivatives of **CB**[*n*].^{3,17–23} Even today, the synthesis of homologues mainly provides **CB**[5], **CB**[7], **CB**[8], and **CB**[10], and the synthesis of derivatives of **CB**[*n*] is limited to the smaller ring sizes (Me₁₀**CB**[5], Cy₅**CB**[5], Cy₆**CB**[6], and Ph₂**CB**[6]). Despite these limitations, it has become increasingly clear that the homologues and derivatives of **CB**[*n*] have superior characteristics.^{3,17–22} The complexity of the **CB**[*n*] synthesis — the formation of *n* rings, 2*n* methylene bridges, and control over the relative stereochemistry of *n* glycoluril

rings — has made investigations of the mechanism of **CB**[*n*] synthesis challenging. Such investigations can, however, provide insights that expand the scope and define the limitations of **CB**[*n*] synthesis.

The use of methylene bridged glycoluril dimers as a model system for **CB**[*n*] synthesis has reduced the complexity of the investigation to the formation of one ring, two methylene bridges, and control over the relative stereochemistry of two glycoluril rings. This reduction in complexity has allowed us to probe the mechanism of **CB**[*n*] formation at a level of detail that has not been possible to date. Specifically, we have demonstrated that the condensation reactions that connect two glycoluril rings by methylene bridges deliver both the S-shaped and the C-shaped diastereomers as kinetic products. The relative thermodynamic stability of these two diastereomers was examined by separately resubmitting the pure C- and S-shaped diastereomers to the reaction conditions. The C-shaped diastereomers are more stable than the corresponding S-shaped diastereomers by 1.55–3.25 kcal mol⁻¹. The values of Δ*G* are only modestly solvent dependent. These measurements represent the first experimental determinations of the driving force for the C- to S-equilibrium which is important in the conversion of the growing methylene bridged glycoluril oligomer into the all C-shaped **CB**[*n*]. The mechanism of this S- to C-interconversion was delineated by a series of labeling experiments. These experiments, performed under anhydrous conditions in ClCH₂-CH₂Cl, establish the intramolecular nature of the isomerization and demonstrate the retention of configuration of the two halves of the dimer. The elucidation of the mechanism of the isomerization reaction has broad implications for the improved synthesis of **CB**[*n*]. For example, the intramolecular nature of the isomerization suggests that it is the length of the growing methylene bridged glycoluril oligomer chain (**4** and **5**) that controls the size of the **CB**[*n*] oligomer. It further suggests that the substitution pattern of these intermediate oligomers might be preserved in **CB**[*n*] oligomers. For example, the heterodimerization of **39e** and **1a** could yield **CB**[*n*] derivative **40** with alternating substituents.¹⁹ Armed with these new insights into the mechanism of **CB**[*n*] formation, it should be possible to expand the range of **CB**[*n*] homologues and **CB**[*n*] derivatives and to capitalize on their superior molecular recognition characteristics.

Experimental Section

General. Starting materials were purchased from Alfa-Aesar, Acros, and Aldrich and were used without further purification. Compounds **6C**–**10C**, **8S**, **12C**, **12S**, **13C**, **13S**, **14CC**, (±)-**14CT**, (±)-**14SC**, **14ST**, **15CC**, (±)-**15CT**, (±)-**15SC**, **15ST**, **16C**–**18C**, **16S**–**18S**, **19**, **20**, **21**, (±)-**22**, and (±)-**23** were prepared according to literature procedures.^{24,31,32} THF and toluene were distilled from sodium benzophenone ketyl, and methylene chloride was distilled from CaH₂ immediately before use. TLC analysis was performed using precoated glass plates from Analtech or Merck. Column chromatography was performed using silica gel (230–400 mesh, 0.040–0.063 μm) from E. Merck using eluents in the indicated v:v ratio. Melting points were measured on a Meltemp apparatus in open capillary tubes and are uncorrected. IR spectra were recorded on a Nicolet Magna spectrophotometer as KBr pellets or thin films on NaCl plates and are reported in cm⁻¹. NMR spectra were measured on Bruker AM-400 and DRX-400 instruments operating at 400 MHz for ¹H and 100 MHz for ¹³C. Mass spectrometry was performed using a VG 7070E magnetic sector instrument by electron impact (EI) or by fast atom bombardment (FAB) using the

indicated matrix. The matrix “magic bullet” is a 5:1 (w:w) mixture of dithiothreitol:dithioerythritol. Electrospray mass spectrometry experiments were performed on a Finnegan LCQ ion-trap mass spectrometer. Elemental analyses were performed by Midwest MicroLab (Indianapolis, IN).

Representative Procedure from Scheme 2. Synthesis of 14ST and (±)-14SC. A mixture of PTSA (737 mg, 3.88 mmol) and $\text{ClCH}_2\text{CH}_2\text{Cl}$ (30 mL) was heated under N_2 at reflux for 30 min under an addition funnel filled with molecular sieves (4 Å). Compounds (±)-**23** (418 mg, 0.78 mmol) and (±)-**22** (385 mg, 0.78 mmol) were added, and heating was continued for 4 h at 60 °C. The reaction mixture was diluted with EtOAc (500 mL), washed with saturated Na_2CO_3 , dried over anhydrous MgSO_4 , and concentrated. Flash chromatography (SiO_2 , $\text{CHCl}_3/\text{CH}_3\text{CN}$, 10:1 and then 4:1) yielded **14ST** (27 mg, 0.03 mmol, 7%), (±)-**14SC** (23 mg, 0.02 mmol, 6%), (±)-**14CT** (48 mg, 0.05 mmol, 12%), and **14CC** (72 mg, 0.07 mmol, 18%) as white solids along with unreacted starting materials (±)-**23** and (±)-**22**. Compound **14ST** (eluted with $\text{CHCl}_3/\text{CH}_3\text{CN}$ 10:1). mp 145–147 °C. TLC ($\text{CHCl}_3/\text{CH}_3\text{CN}$ 10:1): R_f 0.24. IR (KBr, cm^{-1}): 2985m, 2935w, 2842w, 1742s, 1699s, 1457m, 1429s, 1388m, 1368w, 1268s, 1173s, 1030s. ^1H NMR (400 MHz, CDCl_3): 7.42 (d, $J = 8.9$, 2H), 6.72 (d, $J = 8.9$, 2H), 5.67 (d, $J = 16.3$, 2H), 5.52 (d, $J = 16.3$, 2H), 5.06 (d, $J = 13.6$, 2H), 4.95 (d, $J = 13.6$, 2H), 4.22 (d, $J = 16.3$, 2H), 4.19 (q, $J = 7.1$, 4H), 3.96 (d, $J = 16.3$, 2H), 3.84 (s, 6H), 3.85–3.70 (m, 4H), 1.26 (t, $J = 7.1$, 6H), 1.13 (t, $J = 7.1$, 6H). ^{13}C NMR (100 MHz, CDCl_3): 165.4, 164.0, 156.5, 155.2, 155.0, 137.1, 133.2, 127.1, 115.1, 113.0, 81.0, 78.7, 63.7, 63.5, 56.6, 51.9, 44.4, 36.6, 14.0, 13.6. MS (FAB, Magic Bullet): m/z 1019 (100, $[\text{M} + \text{H}]^+$). HR-MS (FAB, Magic Bullet): m/z 1149.0247 ($[\text{M} + \text{Cs}]^+$, $\text{C}_{40}\text{H}_{42}^{79}\text{Br}_2\text{N}_8\text{O}_{14}\text{Cs}$ calcd 1149.0242). Compound (±)-**14SC** (eluted with $\text{CHCl}_3/\text{CH}_3\text{CN}$ 10:1). mp 144–146 °C. TLC ($\text{CHCl}_3/\text{CH}_3\text{CN}$ 10:1): R_f 0.18. IR (KBr, cm^{-1}): 2978w, 2939m, 2842m, 1742s, 1457m, 1429m, 1388s, 1367m, 1309m, 1269s, 1078s, 1020s. ^1H NMR (400 MHz, CDCl_3): 7.42 (d, $J = 8.9$, 2H), 6.72 (d, $J = 8.9$, 2H), 5.64 (d, $J = 16.2$, 2H), 5.56 (d, $J = 16.2$, 2H), 5.01 (s, 2H), 4.99 (s, 2H), 4.32 (d, $J = 16.2$, 2H), 4.25–4.10 (m, 4H), 3.84 (s, 6H), 3.90–3.70 (m, 6H), 1.26 (t, $J = 7.1$, 6H), 1.14 (t, $J = 7.1$, 6H). ^{13}C NMR (100 MHz, CDCl_3): 165.4, 163.9, 156.6, 155.1, 155.0, 137.1, 133.2, 127.2, 114.9, 113.1, 80.9, 78.7, 63.7, 63.5, 56.6, 52.2, 51.5, 44.4, 36.5, 13.9, 13.6. MS (FAB, Magic Bullet): m/z 1019 (100, $[\text{M} + \text{H}]^+$). HR-MS (FAB, Magic Bullet): m/z 1149.0276 ($[\text{M} + \text{Cs}]^+$, $\text{C}_{40}\text{H}_{42}^{79}\text{Br}_2\text{N}_8\text{O}_{14}\text{Cs}$ calcd 1149.0242).

Representative Procedures from Table 1. Isomerization of 12C. A mixture of PTSA (0.042 g, 0.220 mmol) and $\text{ClCH}_2\text{CH}_2\text{Cl}$ (10 mL) was heated under N_2 at reflux for 30 min under an addition funnel filled with molecular sieves (4 Å). Compound **12C** (0.020 g, 0.022 mmol) was added, and reflux was continued for 72 h. The reaction mixture was diluted with EtOAc (100 mL), washed with saturated Na_2CO_3 , dried over anhydrous MgSO_4 , and concentrated. A C:S ratio of 39:1 was calculated on the basis of the integration of the resonances for **12C** (6.06 ppm) and **12S** (5.04 ppm) in the crude ^1H NMR spectrum.

Isomerization of 12S. A mixture of PTSA (0.051 g, 0.220 mmol) and $\text{ClCH}_2\text{CH}_2\text{Cl}$ (10 mL) was heated under N_2 at reflux for 30 min under an addition funnel filled with molecular sieves (4 Å). Compound **12S** (0.050 g, 0.054 mmol) was added, and reflux was continued for 6 days. The reaction mixture was diluted with EtOAc (100 mL), washed with saturated Na_2CO_3 , dried over anhydrous MgSO_4 , and concentrated.

A C:S ratio of 50:1 was calculated on the basis of the integration of the resonances for **12C** (6.06 ppm) and **12S** (5.04 ppm) in the crude ^1H NMR spectrum.

General Procedures for Table 2. Isomerization of 16C. A mixture of PTSA (41 mg, 0.22 mmol) and solvent (6 mL) was heated under N_2 at reflux for 30 min under an addition funnel filled with molecular sieves (4 Å). Compound **16C** (50 mg, 0.045 mmol) was added, and reflux was continued for several days. The reaction mixture was diluted with EtOAc (100 mL), washed with saturated Na_2CO_3 , dried over anhydrous MgSO_4 , and concentrated. The **16C:16S** ratio was calculated on the basis of the integrals of the resonances for **16C** (6.04 ppm) and **16S** (4.98 ppm) in the crude ^1H NMR spectrum.

Isomerization of 16S. A mixture of PTSA (41 mg, 0.22 mmol) and solvent (6 mL) was heated under N_2 at reflux for 30 min under an addition funnel filled with molecular sieves (4 Å). Compound **16S** (50 mg, 0.045 mmol) was added, and reflux was continued for several days. The reaction mixture was diluted with EtOAc (100 mL), washed with saturated Na_2CO_3 , dried over anhydrous MgSO_4 , and concentrated. The **16C:16S** ratio was calculated on the basis of the integrals of the resonances for **16C** (6.04 ppm) and **16S** (4.98 ppm) in the crude ^1H NMR spectrum.

Representative Procedure from Scheme 4. Isomerization of (±)-14SC. A mixture of PTSA (23 mg, 0.12 mmol) and $\text{ClCH}_2\text{CH}_2\text{Cl}$ (6 mL) was heated under N_2 at reflux for 30 min under an addition funnel filled with molecular sieves (4 Å). Compound (±)-**14SC** (15 mg, 0.02 mmol) was added, and heating was continued for 12 days. The reaction mixture was diluted with EtOAc (100 mL), washed with saturated aqueous Na_2CO_3 , dried over anhydrous MgSO_4 , and concentrated. The ^1H NMR spectrum of the crude material was used to calculate a CT:SC ratio of 15:1 on the basis of the integrals of the resonances for (±)-**14CT** at 6.03 ppm and (±)-**14SC** at 5.01 ppm.

X-ray Crystal Structure of 18C. A detailed description of the data collection, solution, and refinement of the structure can be found in the Supporting Information. Crystal data for **18C**: $[\text{C}_{38}\text{H}_{32}\text{N}_8\text{O}_{12}\text{F}_8]$ - $[\text{C}_7\text{H}_8]$ (1036.85); orthorhombic, space group $Pca2(1)$; colorless block, $a = 16.1489(10)$ Å, $b = 11.4856(7)$ Å, $c = 24.0250(15)$ Å; $V = 4456.2(5)$ Å³; $Z = 4$; $T = 193(2)$ K; $R(F) = 0.0451$; GOF on $F^2 = 1.044$.

AM1 Calculations. All computations were performed on a Dell Precision 620 workstation with 512 MB of RAM and dual Pentium III processors running PC Spartan Pro under Windows 2000 professional. The overall structure was created with Spartan’s graphical user interface and then minimized by MMFF94 or SYBYL molecular mechanics calculations. These minimized structures served as the input files for the AM1 calculations.

Acknowledgment. We thank the National Institutes of Health (GM61854) and the University of Maryland for generous financial support. We thank Professor Bruce Jarvis for helpful discussions. L.I. is a Cottrell Scholar of Research Corp.

Supporting Information Available: Experimental procedures and spectral data for all new compounds, and details of the X-ray crystallographic analysis of **18C** (PDF). This material is available free of charge via the Internet at <http://pubs.acs.org>.

JA025876F